Appl. Phys. B 83, 651–657 (2006)
DOI: 10.1007/s00340-006-2259-1

Applied Physics B
Lasers and Optics

K. AMAL[1]
S.H. ELNABY[1]
V. PALLESCHI[2]
A. SALVETTI[2]
M.A. HARITH[1,✉]

Comparison between single- and double-pulse LIBS at different air pressures on silicon target

[1] National Institute of Laser Enhanced Science (NILES), Cairo University, Giza, Egypt
[2] IPCF-CNR, Applied Laser Spectroscopy Laboratory, Pisa, Italy

Received: 16 May 2005/Final version: 27 March 2006
Published online: 5 May 2006 • © Springer-Verlag 2006

ABSTRACT A comparative study between single- and double-pulse laser-induced breakdown spectroscopy (LIBS) was performed on an *n*-type silicon(111) target. A new mobile double-pulse instrument for LIBS analysis was used for the measurements. The experiment was carried out at different air pressures of 0.7, 470 and 1000 hPa. It has been found that, in the case of double-pulse LIBS, the emission intensities of atomic and ionic lines are strongly enhanced at higher pressures. Using Stark broadening of the atomic lines of silicon, it was found that the electron number densities for single and double pulses are approximately the same ($N_e \sim 10^{17}$ cm^{-3}). Plasma excitation and ionization temperatures were determined from a Boltzmann plot. The double-pulse laser-induced plasma was studied at different interpulse delay times of 1, 2, 5, 10, 15, 25 and 50 μs. The results indicated that the interaction between the laser, plasma and target gives higher atomic and ionic intensities at shorter interpulse delay times.

PACS 52.38.Mf; 79.20.Ds; 52.50.Jm

1 Introduction

The interaction of laser radiation with solid targets is involved in a large variety of applications, including plasma characterization, laser ablation [1], thin film study applications and depth profiling [2]. In particular, laser-induced plasma spectroscopy (LIPS) is considered one of the most promising analytical techniques, since its first introduction in the second half of the twentieth century [3]. In analytical atomic spectroscopy, LIPS has been frequently used and proposed for atomic emission spectrometry. In this case the technique is most often referred to as laser-induced breakdown spectrometry (LIBS) [4]. In its original version, LIBS analysis used a single laser pulse, that is, the plasma on the target was produced by a single laser shot directed onto the sample surface. Even in this relatively simple configuration, the interaction of laser radiation with a solid target is a complex phenomenon, up to now not completely understood and still under intensive investigation. In addition, it is difficult to obtain suitable standards, because of interference effects (the matrix effect). Conventional (single-pulse) LIBS has consequently a poorer sensitivity than several competing atomic spectroscopic techniques such as inductively coupled plasma atomic emission spectrometry (ICP-AES) or inductively coupled plasma mass spectroscopy (ICP-MS) [4]. In recent years, one way to overcome these problems was proposed through the use of double-pulse LIBS, when two lasers or two pulses from one laser, separated by a delay time of the order of microseconds, are used. Double-pulse LIBS was first applied to the analysis of liquid samples, then solids immersed in liquids [5–7]. In recent years, double-pulse LIBS has also been extensively applied to the analysis of solid samples in a gaseous or ambient air environment [8–16].

Different geometrical configurations are used in double-pulse LIBS. In the so-called 'collinear' configuration, the two laser pulses have the same axis of propagation and are both directed orthogonally to the sample surface [8, 12–16]. Studies of collinear double pulses were performed by Sattmann et al. [12–14] using a single Nd:YAG laser capable of emitting two sequential pulses. The authors compared the double-pulse results with the ones obtained using a single pulse with the same energy of the two combined laser pulses.

St-Onge et al. [8] investigated the physical properties and emission yield of the plasma formed from solid Al alloys in air in a collinear double-pulse configuration, using a Nd:YAG laser operated in double-pulse mode at the fundamental wavelength (1064 nm). They found that the Al II line at 281.6 nm is enhanced when using two sequential laser pulses instead of a single pulse of equal energy. However, the electron density was found to be approximately the same for both the single and double pulses and the plasma temperature was less than 10% higher in the double-pulse configuration. The effect of the interpulse interval on the plasma emission was also studied. The other common configuration of double-pulse LIBS is the 'orthogonal' configuration, where the two laser beams are orthogonal to each other. In this case, the laser parallel to the target comes first, producing preablation plasma in air [9, 10], or after the perpendicular one, causing reheating and excitation of the already ablated material [11]. Angel et al. [10] proposed a perpendicular preablation setup using two Nd:YAG lasers. The first pulse was directed parallel to the sample and produced a preablation

✉ Fax: +202-5675335, E-mail: mharithm@egypt.com

spark in air, while the second beam, delayed after the pre-ablation spark by several microseconds, was directed perpendicular to the sample to induce the formation of the plasma from the sample. This arrangement led to a large increase of the line intensity (sometimes up to 40 fold). The authors attributed this enhancement to an increase in ablation efficiency.

The evolution of the plasma obtained in orthogonal and collinear configurations is expected to be different, since the temporal orders of ablation and excitation processes in the plume are, in turn, different. Both perpendicular and collinear configurations have been extensively tested and the results obtained suggest that the use of the double-pulse technique could improve the analytical capabilities of the LIBS technique, through an enhancement of the spectral signal to noise ratio in the obtained spectra.

In recent years, only a few papers were published on the dependence of the double-pulse LIBS signal on the ambient gas used. A reheating perpendicular double-pulse experiment was performed by Uebbing et al. [11] at reduced pressure of argon buffer gas. It was found that the proper choice of the ambient gas conditions resulted in an improvement in the reproducibility of the measurements and accuracy of the calibration curves built by internal standardization.

Cristoforetti et al. [15, 16] studied the effect of ambient gas pressure on laser-induced brass plasma in both single- and double-pulse collinear arrangements using two Nd:YAG lasers at the fundamental wavelength. The air pressures considered ranged from around 0.15 hPa to atmospheric conditions. In all experimental conditions, the temperature and the electron density were estimated at two interpulse times of 0.7 and 2 μs. It was found that a 130-hPa ambient gas pressure is the best condition for obtaining a compromise between a large amount of ablated matter and a high temperature, resulting in the highest emission signal. However, the reasons why the double-pulse technique produces such strong enhancement of the line emissions are not completely explained. Most of the above literature and other papers too [17, 18] attributed the observed enhancement to a higher ablation efficiency achieved in double-pulse LIBS experiments. The aim of the present work is thus to study the enhancement effect due to double pulses compared to the single pulse on a Si target at several ambient air pressures. The effect of different experimental parameters and the physical properties of the laser-induced plasma of silicon will also be investigated in order to interpret the obtained results.

2 The experimental setup

The experiment was performed using MODI (mobile dual-pulse instrument), a new double-pulse instrument for LIBS analysis produced by Marwan Technology (Italy) in collaboration with the Applied Laser Spectroscopy Laboratory at IPCF-CNR in Pisa. The system, which has been designed for in situ LIBS measurements, incorporates a Nd:YAG laser source, emitting at 1064 nm, operating in single- and double-pulse regimes. The laser has two rods pumped by the same flash lamp; the delay between the two laser pulses can be varied from 0 (single pulse) to 60 μs. The interpulse delay between the two pulses is controlled by a delay unit included in the laser control system (see Fig. 1).

The two pulses are emitted in a collinear arrangement and focused on an *n*-type silicon(111) target to form plasma into a vacuum-tight chamber. The energy of the two pulses was fixed to 55 mJ per pulse measured by means of a Scientech power meter and monitored by an oscilloscope through a fast photodiode.

The laser beams were focused on the Si target using a 10-cm focal length lens. The target was mounted on an *X*–*Y* micrometric translation stage, remotely controllable by a personal computer (PC).

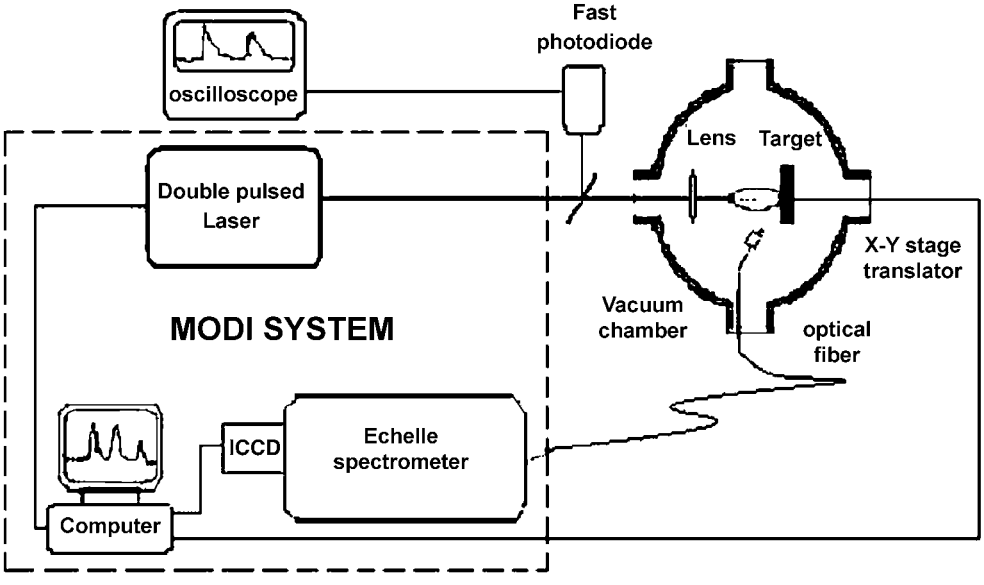

FIGURE 1 Experimental setup

The plasma optical emission was collected by a quartz optical fiber with a diameter of 1 mm inserted into the chamber and held at a distance of 2 cm above the plasma, to ensure that the radiation from the whole plasma is detected at all pressures considered. The direction of observation was fixed at an angle of 30° with respect to the target surface. The plasma emission collected by the optical fiber was sent into an echelle spectrometer (f-number = 5.8) coupled with an intensified CCD for dispersion and detection of the spectral emission of the plasma. The obtained LIBS spectra were then displayed and stored on the personal computer. The same PC was used to control the delay between the laser firing time and the spectral acquisition time, as well as the duration of the acquisition gate. The experiment was done at different interpulse times between the two laser pulses ($\Delta t = 0$, 1, 2, 5, 10, 15, 25 and 50 μs), where $\Delta t = 0$ means two simultaneous pulses, which are equivalent to a single laser pulse of 110-mJ total energy. The acquisition delay time was set at 1 μs after the second pulse with an acquisition gate of 2 μs.

The measurements were performed at different air pressures of 0.7, 470 and 1000 hPa. The pressure in the chamber was measured by a pressure gauge at higher pressures (470 and 1000 hPa), and by a Pirani probe at 0.7 hPa.

3 Results and discussion

Comparison of the spectral emission for single and double pulses at different interpulse times $\Delta t = 1$, 2, 5, 10, 15, 25 and 50 μs was performed at three ambient air pressures (0.7 hPa, 470 hPa and 1000 hPa). At 0.7 hPa (Figs. 2 and 3), the intensity of the Si I line at 250.6 nm decreases with the interpulse delay Δt. The intensity of the same line is always lower than the one obtained with a single pulse of the same total energy. At 470 hPa an enhancement of the LIBS intensity by a factor ∼ 1.8–1.1 is observed at $\Delta t = 1$ and 2 μs, with respect to that of the single pulse, while there is a drop at longer interpulse delays. Finally, at 1000 hPa the enhancement in LIBS intensity is clear for the interpulse intervals $\Delta t = 1, 2, 5,$ 10 and 15 μs, while there is a drop in intensity at $\Delta t = 25$ and 50 μs. An enhancement by a factor of about three is reached at $\Delta t = 1$ μs, as shown in Fig. 3.

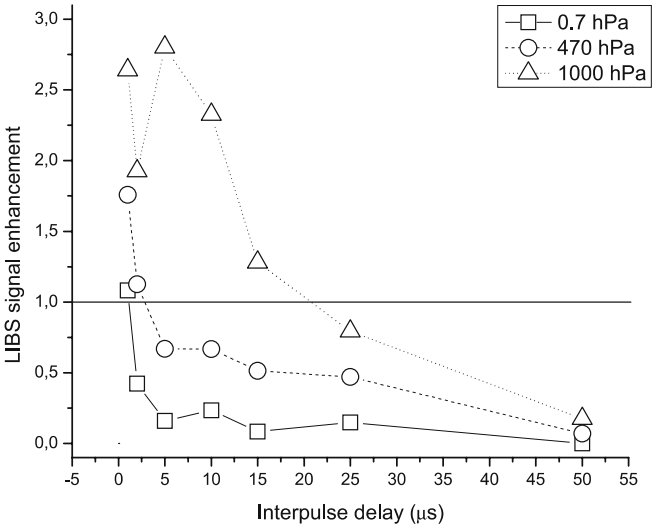

FIGURE 3 LIBS signal enhancement for the Si I line at 250.6 nm, as a function of the interpulse delay at 0.7 (*squares*), 470 (*circles*) and 1000 (*triangles*) hPa

A similar behavior is also observed for the ionized silicon lines at 504.1 and 634.7 nm. At low pressures (0.7 hPa) the LIBS signal decreases at all the interpulse delays (Figs. 4 and 5). Also, at 470 hPa there is no enhancement with the interpulse delay. However, at high pressure (1000 hPa) an enhancement by a factor from two to five is observed at short interpulse delays ($\Delta t = 1$, 2 and 5 μs). It is noticeable that the maximum LIBS signal is observed, both for neutral and ionic silicon lines, at 470 hPa and at a short interpulse delay ($\Delta t = 1$ μs).

Note that the strong LIBS signal enhancement at 1000 hPa is also due to the drop of the single-pulse emission intensity with respect to the value observed at 470 hPa (see Fig. 6).

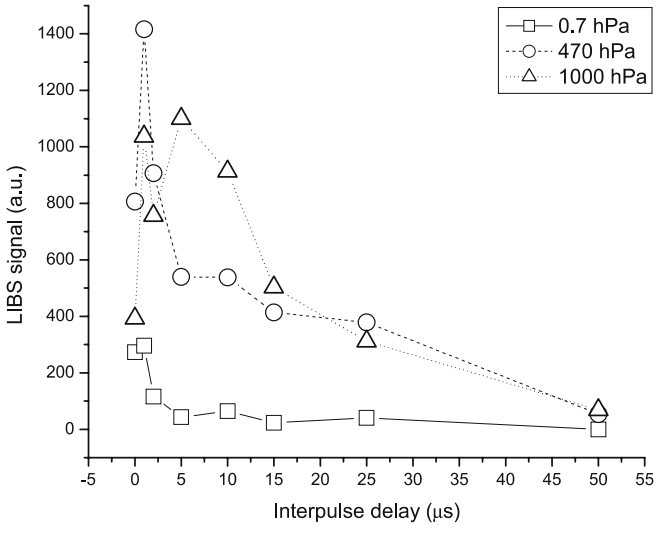

FIGURE 2 LIBS signal from Si I line at 250.6 nm, as a function of the interpulse delay ($\Delta t = 0$ corresponds to single pulse) at 0.7 (*squares*), 470 (*circles*) and 1000 (*triangles*) hPa

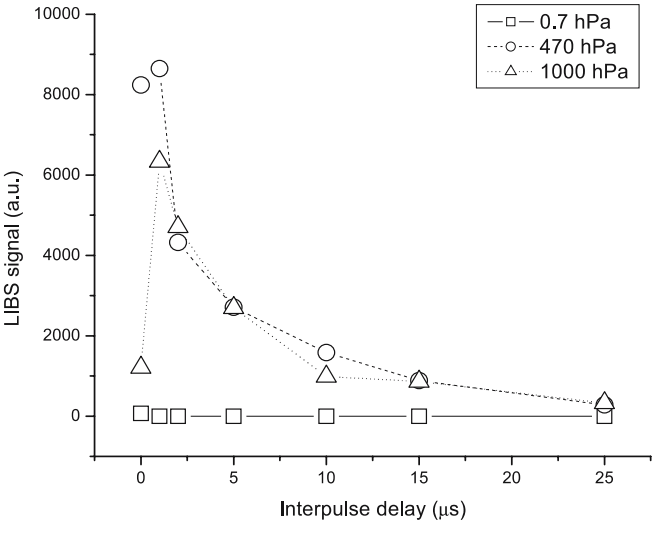

FIGURE 4 LIBS signal from Si II line at 634.7 nm, as a function of the interpulse delay ($\Delta t = 0$ corresponds to single pulse), at 0.7 (*squares*), 470 (*circles*) and 1000 (*triangles*) hPa

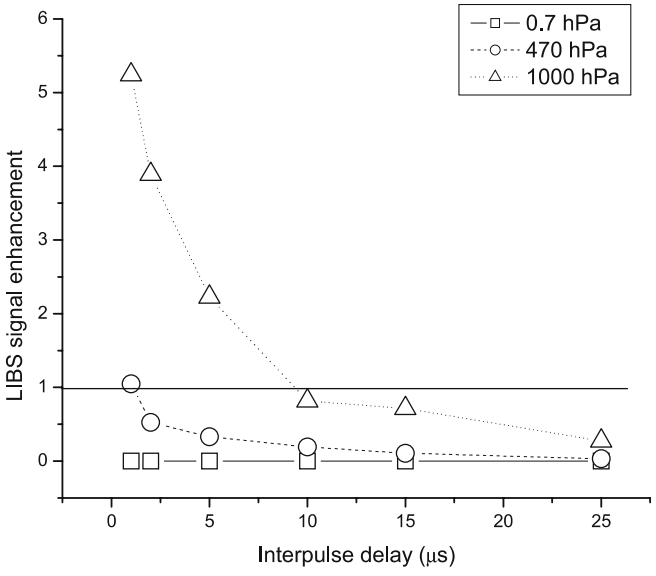

FIGURE 5 LIBS signal enhancement for the Si II line at 634.7 nm, as a function of the interpulse delay at 0.7 (*squares*), 470 (*circles*) and 1000 (*triangles*) hPa

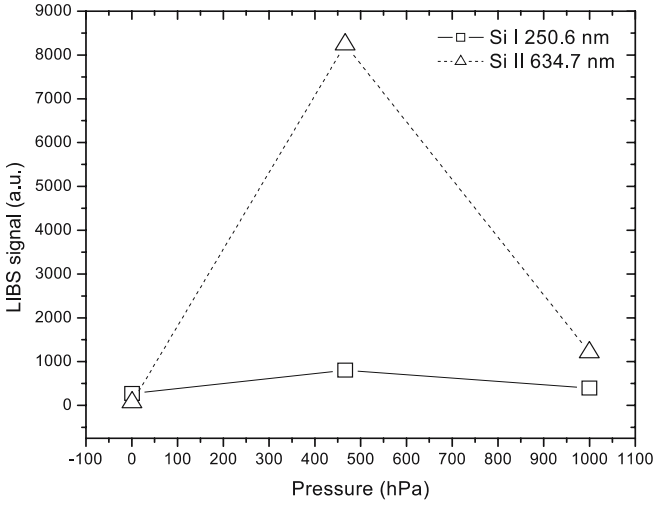

FIGURE 6 Dependence of single-pulse LIBS signal as a function of the ambient gas pressure, for the Si I line at 250.6 nm (*squares*) and the Si II line at 634.7 nm (*triangles*)

3.1 *Pressure and interpulse time effect*

The relation between LIBS signal, air pressure and interpulse interval is quite complex. The intensity dependence of LIBS lines on air pressure, in single-pulse configuration, was firstly reported by Sdorra and Niemax [19]. The same behavior was also observed in previous works [15, 16] for the Cu I line at 521.5 nm at different air pressures, ranging from 0.15 hPa to atmospheric pressure, where the maximum intensity was observed at 135 hPa.

The non-monotonic dependence of the line intensity with ambient gas pressure shown in Fig. 6 is in good agreement with the findings of the above-mentioned references. This was not a priori evident, since different behaviors have been reported for the double-pulse effect in different metals, soils or ceramic material [20, 21]; from here in fact came our motivation in studying the ambient gas pressure effect on double-pulse LIBS in silicon.

The behavior observed in Fig. 6 can be attributed to the effect of laser shielding. The absorption of the laser pulse by the produced plasma prevents part of the laser energy from reaching the target. This effect is particularly important when using the fundamental (IR) wavelength. At low pressure (0.7 hPa) laser shielding is very low and so most of the laser energy reaches the target, resulting in a large mass removal and, consequently, an increase of the number of emitting atoms. However, because of the low absorption of the laser energy by the plasma, the plasma temperature is quite low, and the resulting LIBS intensity is also relatively low. The reverse is true at high pressure (1000 hPa) where the plasma temperature is relatively high, because of the laser absorption by the plasma, but the ablated mass is lower because of the laser shielding effect. The balance between these two effects produces a maximum in the single-pulse LIBS signal at intermediate pressures (in our case, 470 hPa). According to the results of Cristoforetti et al. [15, 16], laser shielding is reduced in the case of double pulses, in particular for short interpulse intervals and even at higher ambient gas pressures (for example 1000 hPa).

Figures 7 and 8 depict plasma emission intensities versus the air pressure at different laser interpulse delays (1 up to 50 μs), for the Si I line at 250.6 nm and the Si II line at 634.7 nm. For the neutral line, at interpulse delays between $\Delta t = 5$ and 15 μs, the LIBS intensity increases as the air pressure increases from 0.7 to 1000 hPa; a similar behavior is observed for the Si II line, although the LIBS signal does not change too much from 470 to 1000 hPa at interpulse delays between $\Delta t = 1$ and 10 μs. The enhancement of the LIBS signal with respect to the single pulse, as a function of the ambient pressure, is shown in Figs. 9 and 10 for the Si I and Si II lines considered here. The enhancement of the LIBS signal with pressure is attributed to changes in the surrounding atmosphere produced by the first laser pulse [15–18]. As the first plasma is induced, atoms rush out of the target surface at supersonic speed, pushing the surrounding gas like a piston. These fast-moving

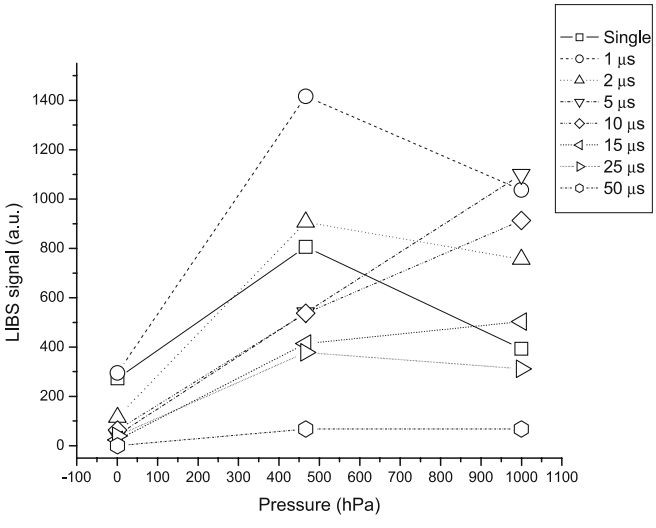

FIGURE 7 LIBS signal from Si I line at 250.6 nm, as a function of the ambient gas pressure for different interpulse delays

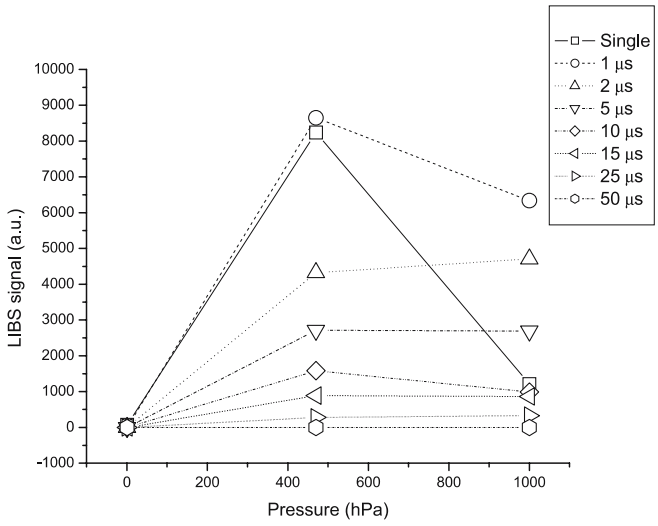

FIGURE 8 LIBS signal from Si II line at 634.7 nm, as a function of the ambient gas pressure for different interpulse delays

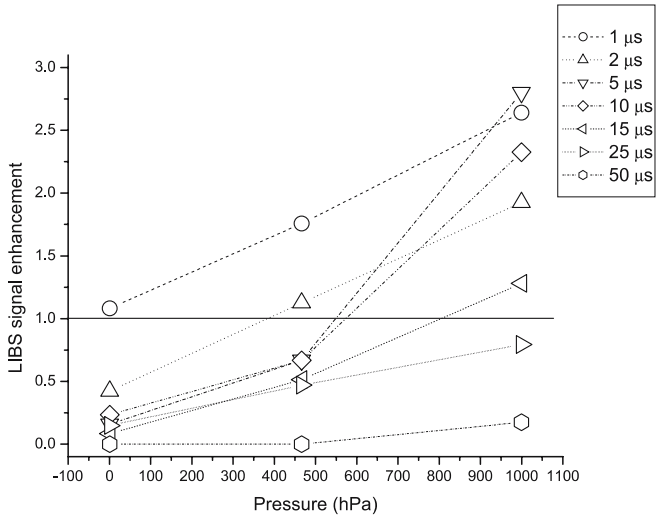

FIGURE 9 LIBS signal enhancement of the Si I line at 250.6 nm, as a function of the ambient gas pressure for different interpulse delays

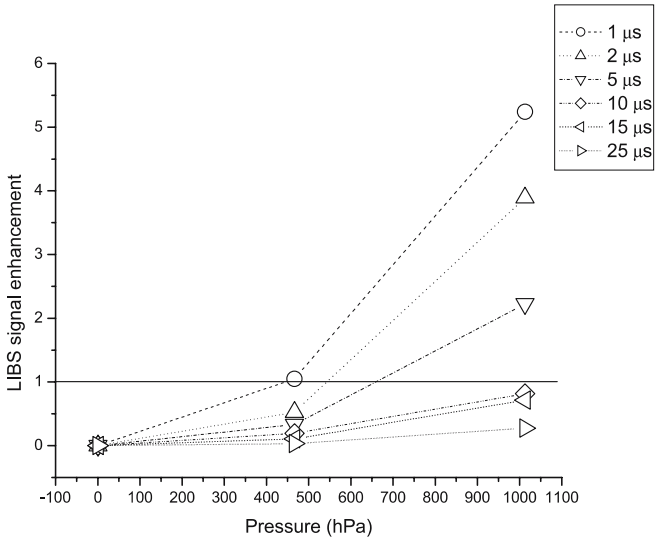

FIGURE 10 LIBS signal enhancement of the Si II line at 634.7 nm, as a function of the ambient gas pressure for different interpulse delays

atoms, interacting with the surrounding gas, give rise to a compression process. As a result of this compression, a shock wave is generated in the surrounding gas. Sedov theory [22] predicts that the shock-wave front is characterized by a large mass density pileup, while behind it a rarefied gas is left. The plasma induced by the second pulse occurs in the environment produced by the first pulse, which is characterized by a reduction of the laser shielding effect. Therefore, the second laser pulse is less absorbed and most of its laser energy reaches the target surface, thus producing a higher mass removal that in turn increases the LIBS intensity.

Moreover, at longer interpulse delays ($\Delta t = 25$ and 50 μs), the enhancement of the LIBS signal is less than 1 at all the pressures considered (i.e. the double-pulse LIBS signal is lower than the one obtained using a single pulse of the same energy). The noticed lowering in intensity at these intervals could be explained according to the long time elapsed between the two pulses. In fact, after such a relatively long delay time, the shock wave produced by the first laser pulse weakens and nearly disappears before the arrival of the second laser pulse. This means that the second laser pulse will induce a new plasma plume in circumstances similar to the single-pulse configuration; however, the laser energy in this case is lower (one-half) of the single-pulse case and consequently the emitted intensity is lower. Such an effect of a long interpulse has been studied before; for example, Yamamoto et al. [23] used multiple pulses (8–9 pulses) each separated by 20–30 μs to analyze metal contaminants on solid surfaces. It turned out that the emission yield was similar to the summation of the emissions from several distinct laser-induced plasmas. This phenomenon is consistent with the interpretation given above for the LIBS signal enhancement in terms of a reduction of the effective ambient pressure produced by the first shock wave.

3.2 *Plasma parameters*

The determination of plasma parameters (electron density and electron temperature) is essential for the comprehension of the mechanisms underlying the double-pulse LIBS technique. The local thermodynamic equilibrium (LTE) approximation is often used for modeling the plasma in both configurations. One of the crucial parameters for the establishment of LTE conditions is the plasma electron density, since a necessary condition for LTE is given by the McWhirter criterion

$$n_{\mathrm{e}}(\mathrm{cm}^{-3}) \geq 1.4 \times 10^{14} (kT)^{1/2} \Delta E^3 \,, \tag{1}$$

where T (in eV) is the plasma temperature and ΔE (in eV) is the energy difference between upper and lower levels of the transition.

Although a high electron density is essential for establishing the equilibrium, its calculation does not rely on the assumption of LTE. Plasma electron density is usually measured from the determination of the Stark broadening of the emission lines (see Griem [24]), using the approximate formula

$$n_{\mathrm{e}} = \Delta\lambda_{1/2} / 2w_{\mathrm{S}} \times 10^{16} \,, \tag{2}$$

where $\Delta\lambda_{1/2}$ is the FWHM of the emission line and w_S is the Stark coefficient. The dependence on plasma temperature of the Stark coefficient is usually neglected, since the variations expected are typically of the order of 10%. Figure 11 shows the behavior of the electron density against the interpulse separation at air pressures of 0.7, 470 and 1000 hPa; the emission line used for the Stark broadening measurements was the Si I line at 250.6 nm. The electron density is very similar for both 470 and 1000 hPa. However, at 470 hPa the electron density is slightly higher than at 1000 hPa at $\Delta t = 0$ and 1 μs; this behavior is reversed at higher interpulse delays ($\Delta t = 5$, 10, 15, 25 and 50 μs). At the air pressure of 0.7 hPa there is a lowering in the electron density compared to 470 and 1000 hPa, except for very short delays ($\Delta t = 0$ and 1 μs). In any case, the electron densities measured at all the pressures and interpulse delays are consistent with the McWhirter criterion. It should be noted, however, that the fulfillment of the McWhirter criterion does not guarantee LTE equilibrium, especially in low-pressure conditions where the expansion of the plasma might be too fast for the establishment of thermal equilibrium.

If LTE is verified in the plasma, the population density of atomic states is well described by the Boltzmann distribution and the plasma temperature can be deduced using the usual Boltzmann plot method. However, the conditions required for thermometric purposes (lines emitted from the same species, in close spectral proximity, reasonably intense, of known transition probability and with very different upper energy levels) were difficult to meet due to the small number of silicon lines clearly defined [25]. As an alternative to the Boltzmann plot method, when the electron density of the plasma is independently measured, the Saha–Boltzmann technique can be used.

In fact, in the LTE approximation the population of the ith energy level is given by

$$n_i = N g_i \frac{\mathrm{e}^{-E_i/kT}}{U(T)} , \tag{3}$$

where N is the number of atoms or ions, g_i is the ith level degeneracy, k is the Boltzmann constant and $U(T)$ is the partition function for the emitting species, which depends on the plasma temperature T.

The equilibrium between neutral and ionized atoms in the plasma is governed by the Saha equation

$$n_\mathrm{e} \frac{N^\mathrm{II}}{N^\mathrm{I}} = 6 \times 10^{21} \frac{g^\mathrm{II}}{g^\mathrm{I}} (kT)^{3/2} \mathrm{e}^{-E_\mathrm{ion}/kT} , \tag{4}$$

where n_e is the plasma electron density (in cm^{-3}), E_ion is the ionization energy and the superscripts I and II refer to the neutral and ionized states, respectively. Equations (3) and (4) can be combined together for deriving the plasma temperature using the so-called Saha–Boltzmann plot method described, for example, by Yalcin et al. [26]. According to this method, both neutral and ionic lines are used for the determination of plasma temperature, thus improving the precision of the calculation with respect to the usual Boltzmann plot method, where the single species of the same element are treated separately.

In the present conditions, the measured electron densities should guarantee that the use of the Boltzmann and Saha equations would give a reasonable estimate of the plasma temperature, with the usual caveat that, if the LTE approximation is not completely fulfilled, the excitation temperature (the temperature in the Boltzmann equation) might be slightly different from the ionization temperature (the temperature in the Saha equation). However, at this level of the discussion, the fact that slightly different temperatures may be defined in a plasma not exactly at LTE should not give too many problems, at least until the same parameters are compared in single- and double-pulse configurations.

The atomic and ionic lines selected for determining the excitation temperature are listed in Table 1. As shown in Fig. 12, at 470 and 1000 hPa, the calculated temperatures are similar and around 1 eV; no appreciable differences between the values of T for both pressures with the inter-

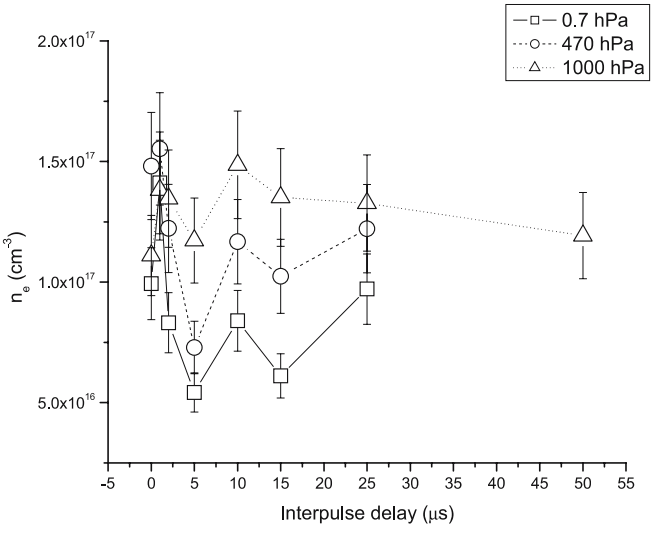

FIGURE 11 Plasma electron density as a function of the interpulse delay, at 0.7 (*squares*), 470 (*circles*) and 1000 (*triangles*) hPa

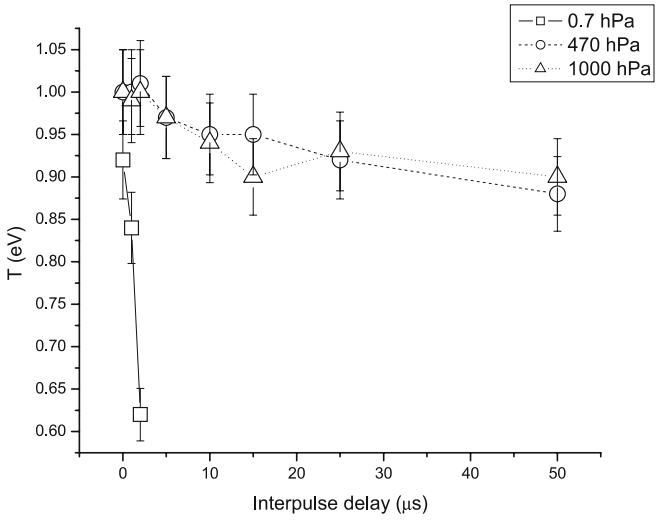

FIGURE 12 Plasma temperature as a function of the interpulse delay, at 0.7 (*squares*), 470 (*circles*) and 1000 (*triangles*) hPa

Species	λ (nm)
Si I	243.5
Si I	253.2
Si I	298.7
Si I	390.5
Si II	504.1
Si II	505.6
Si II	634.7
Si II	637.1

TABLE 1 Silicon emission lines used for the measurement of plasma temperature in Saha–Boltzmann plot

pulse delay are observed, although a slight decrease of the plasma temperature with the interpulse delay is clearly noticeable. At low pressure, however, the plasma temperature is considerably lower and rapidly decreases with the interpulse delay, thus confirming that the effect of a reduced laser shielding is reflected in a reduction of the plasma temperature.

4 Conclusion

A new double-pulse mobile instrument (MODI) was used for studying the effect of air pressure on single- and double-pulse laser-induced plasma on a silicon target. A comparative study between the single and double pulses was performed in the different experimental conditions. The interpulse time between the two pulses was found to be an essential parameter to enhance the efficiency of the double-pulse technique. The characterization of the laser-induced plasma was also completed by determining the plasma temperature and electron density at the different ambient gas pressures and as a function of the interpulse delay. The results obtained are consistent with the interpretation given by previous published works of the enhancement of the LIBS signal obtained in double-pulse experiments in terms of the reduced laser shielding due to the effect of the shock wave produced by the first laser pulse.

REFERENCES

1 R.E. Russo, Appl. Spectrosc. **49**, 14A (1995)
2 D.R. Anderson, C.W. Mcleod, A.T. Smith, Appl. Spectrosc. **49**, 691 (1995)
3 L.J. Radziemski, D.A. Cremers, *Laser-Induced Plasmas and Applications* (Marcel Dekker, New York, 1989)
4 Y.L. Lee, K. Song, J. Sneddon, in *Lasers in Analytical Atomic Spectroscopy*, ed. by J. Sneddon, T.L. Thiem, Y.L. Lee (VCH, New York, 1997), p. 197
5 D.A. Cremers, L.J. Radziemski, T.R. Loree, Appl. Spectrosc. **38**, 721 (1984)
6 R. Nyga, W. Neu, Opt. Lett. **18**, 747 (1993)
7 S. Nakamura, Y. Ito, K. Sone, H. Hiraga, K. Kaneko, Anal. Chem. **68**, 2981 (1996)
8 L. St-Onge, M. Sabsabi, P. Cielo, Spectrochim. Acta B **53**, 407 (1998)
9 D.N. Stratis, K.L. Eland, S.M. Angel, Appl. Spectrosc. **55**, 1297 (2001)
10 S.M. Angel, D.N. Stratis, K.L. Eland, T. Lai, M.A. Berg, D.M. Gold, Fresenius J. Anal. Chem. **369**, 320 (2001)
11 J. Uebbing, J. Brust, W. Sdorra, F. Leis, K. Niemax, Appl. Spectrosc. **45**, 1419 (1991)
12 R. Sattmann, V. Sturm, R. Noll, J. Phys. D Appl. Phys. **28**, 2181 (1995)
13 R. Noll, R. Sattmann, V. Sturm, S. Lungen, H.J. Von Wachtendonk, Stahl Eisen **117**, 57 (1997)
14 R. Noll, R. Sattmann, V. Sturm, S. Winkelmann, J. Anal. At. Spectrom. **19**, 419 (2004)
15 G. Cristoforetti, S. Legnaioli, V. Palleschi, A. Salvetti, E. Tognoni, Spectrochim. Acta B **59**, 1907 (2004)
16 G. Cristoforetti, S. Legnaioli, V. Palleschi, A. Salvetti, E. Tognoni, Appl. Phys. B **80**, 559 (2005)
17 S. Wen, X. Mao, R.E. Russo, Spectrochim. Acta B **60**, 870 (2005)
18 M. Corsi, G. Cristoforetti, M. Giuffrida, M. Hidalgo, S. Legnaioli, V. Palleschi, A. Salvetti, E. Tognoni, C. Vallebona, Spectrochim. Acta B **60**, 872 (2005)
19 W. Sdorra, K. Niemax, Mikrochim. Acta **107**, 319 (1992)
20 L.I. Sedov, *Similarity and Dimensional Methods in Mechanics* (CRC, Moscow, 1993)
21 A. Bertolini, G. Carelli, F. Francesconi, M. Francesconi, L. Marchesini, P. Marsili, F. Sorrentino, G. Cristoforetti, S. Legnaioli, V. Palleschi, L. Pardini, A. Salvetti, Anal. Bioanal. Chem., in press (available online) (2006)
22 C. Gautier, P. Fichet, D. Menut, J. Dubessy, Spectrochim. Acta B, in press (available online) (2006)
23 K.Y. Yamamoto, D.A. Cremers, M.J. Ferris, L.E. Foster, Appl. Spectrosc. **50**, 222 (1996)
24 H.R. Griem, *Plasma Spectroscopy* (McGraw Hill, New York, 1964)
25 M. Milan, J.J. Laserna, Spectrochim. Acta B **56**, 275 (2001)
26 S. Yalcin, D.R. Crosley, G.P. Smith, G.W. Faris, Appl. Phys. B **68**, 121 (1999)